JOURNAL OF ENZYME INHIBITION AND MEDICINAL CHEMISTRY
2018, VOL. 33, NO. 1, 190–198
https://doi.org/10.1080/14756366.2017.1404590

Taylor & Francis
Taylor & Francis Group

RESEARCH PAPER

OPEN ACCESS Check for updates

Synthesis and characterisation of celastrol derivatives as potential anticancer agents

Hong-Jian Zhang*, Guo-Rui Zhang*, Hu-Ri Piao and Zhe-Shan Quan

Key Laboratory of Natural Resources and Functional Molecules of the Changbai Mountain, Affiliated Ministry of Education, College of Pharmacy, Yanbian University, Yanji, Jilin, China

ABSTRACT

In the present study, three series of novel celastrol derivatives were designed and synthesised by modifying the carboxylic acid at the 20th position with amino acid, amine, and triazole derivatives. All the synthesised compounds were screened for their anticancer activities using MTT assay against AGS, MGC-803, SGC-7901, HCT-116, A549, HeLa, BEL-7402, and HepG-2 cell lines. Most of the synthesised compounds exhibited potent antiproliferative effects. The most promising compound 3-Hydroxy-9β,13α-dimethyl-2-oxo-24,25,26-trinoroleana-1(10),3,5,7-tetraen-29-oic amide, *N*-(*R*)-methyl-3-(1*H*-indol-2-yl)propanoate (**11**) showed considerable high anticancer activity against AGS cell lines, with an IC_{50} value of 0.44 μM, and considerably higher activities against HCT-116, BEL-7402, and HepG-2 cell lines, with IC_{50} values of 0.78, 0.63, and 0.76 μM, respectively. The results of apoptosis tests and molecular docking study of compound **11** binding to Caspase-3 revealed that its mechanism of action with antiproliferative was possibly involved in inducing apoptosis by inducing the activation of caspase-3.

ARTICLE HISTORY
Received 17 July 2017
Revised 12 October 2017
Accepted 9 November 2017

KEYWORDS
Synthesis; celastrol; amino acid; triazole; anticancer; docking

Introduction

Celastrol, a quinone methide triterpene, is an active ingredient first extracted from the roots of the Chinese medicinal plant "Thunder of God Vine" (Celastraceae, Tripterygium). A literature survey showed that celastrol can destroy cell lines by activating the classical apoptotic pathway, and it strongly inhibits cell proliferation. It was proven to have several biological activities, such as anticancer[1–4], antifungal[5], antifibrotic[6], anti-inflammatory[7,8], and antioxidant[6,9] activities, and resistance to neurodegenerative disease activity[10]. Although celastrol has important pharmacological activities, it also has several drawbacks such as poor water solubility, high toxicity, poor stability, etc., which restrict its clinical application. Thus, it is very important to improve its solubility and stability and reduce its toxicity by modifying its structure. Previous studies have also suggested that the 20th carboxylic acid position of celastrol can be easily modified[11–14], and the derivatives play an important role in anticancer activity.

Amino acids, the basic biological and functional units of proteins, play an important role in human metabolism. Amino acid derivatives display diverse biological functions, including immunomodulatory[15], antituberculosis[16], antifatigue[17], bactericidal[18], and anticancer[19,20] activities. In general, the solubility of compounds is directly related to the number of polar groups present, such as hydroxyl, carboxyl, amino, amide, etc. A change in activity may be followed by a change in solubility of compounds. Moreover, an amide group would increase the stability of the compound *in vitro and in vivo*, and thus, it would be less susceptible to enzymatic hydrolysis and act as a hydrogen donor. As reported by Csuk et al., compounds containing a triazole moiety bind to a variety of enzymes and receptors by non-covalent interactions; these compounds also have a wide array of biological activities[21]. In the present study, to develop novel celastrol derivatives with potent antitumor bioactivities, we introduced three different groups to the 20th carboxylic acid position of celastrol. We hypothesised that the combination of appropriate amino acids ester, amino, and amide groups with a celastrol core may have increased anticancer activity. In the present study, three series of celastrol derivatives were synthesised, and their antitumor activities were evaluated against eight cancer cell lines (AGS, MGC-803, HCT-116, SGC-7901, BEL-7402, A549, HeLa, and HepG-2). Next, to investigate its possible mechanism of action, the antiproliferative activity of the derivative with the strongest antitumor activity was evaluated.

Experimental

Materials and methods

All reagents were obtained commercially and were used without further purification. Solvents were dried according to standard procedures. Reactions were monitored by thin-layer chromatography (TLC) on silica gel plates. Melting points were determined in open capillary tubes and were uncorrected. ^{1}H NMR and ^{13}C NMR spectra were measured on an AV-300 (Bruker, Switzerland), and all chemical shifts were given in ppm relative to TMS. Mass spectra were measured on a HP1100LC (Agilent Technologies, USA). High resolution mass spectra were measured on an MALDI-TOF/TOF mass spectrometer (Bruker Daltonik, Germany).

CONTACT Zhe-Shan Quan zsquan@ybu.edu.cn College of Pharmacy, Yanbian University, No. 121, JuZi Street, Yanji, Jilin 133000, China; Hu-Ri Piao, piaohuri@yahoo.com.cn Yanbian University College of Pharmacy, Yanji 133002, China
*These authors contributed equally to this work and should be considered co-first authors.

© 2017 The Author(s). Published by Informa UK Limited, trading as Taylor & Francis Group.
This is an Open Access article distributed under the terms of the Creative Commons Attribution License (http://creativecommons.org/licenses/by/4.0/), which permits unrestricted use, distribution, and reproduction in any medium, provided the original work is properly cited.

General procedure for the synthesis of compounds **1–11**

A mixture of celastrol (45 mg, 0.1 mmol), EDC·HCl (43 mg, 0.22 mmol), HOBt (30 mg, 0.22 mmol), TEA (102 μL, 0.3 mmol), and various amino acid esters (0.3 mmol) in CH_2Cl_2 (5.0 ml) was stirred at 0 °C for 8 h. Next, the mixture was washed thrice with water and saline, dried using anhydrous $MgSO_4$, filtered, and concentrated *in vacuo*. The mixture was concentrated and purified by normal-phase column chromatography (dichloromethane:methanol =100:1) to obtain the target compounds **11**.

3-Hydroxy-9β,13α-dimethyl-2-oxo-24,25,26-trinoroleana-1(10),3,5,7-tetraen-29-oicamide,N-methyl acetate (1)

Red solid; yield, 47%; m.p. 104–106 °C; ^{1}H NMR (300 MHz, $CDCl_3$), δ: 7.02 (d, J = 7.4 Hz, 1 H), 6.54 (s, 1 H), 6.35 (d, J = 6.9 Hz, 1 H), 6.29 (s, 1 H), 3.94 (s, 2 H), 3.75 (s, 3 H), 2.47 (d, J = 15.5 Hz, 1 H), 2.22 (s, 3 H), 1.45–1.88 (m, 14 H), 1.45 (s, 3 H), 1.28 (s, 3 H), 1.20 (s, 3 H), 1.15 (s, 3 H), 0.87 (s, 1 H), 0.59 (s, 3 H). ^{13}C NMR (75 MHz, $CDCl_3$), δ: 178.34, 177.87, 170.82, 170.17, 164.76, 146.01, 139.95, 127.41, 119.54, 118.04, 116.99, 52.42, 45.06, 44.37, 42.98, 41.32, 40.33, 39.35, 38.20, 36.33, 34.85, 33.55, 33.48, 31.59, 31.20, 30.80, 30.04, 29.43, 28.66, 21.74, 18.15, 10.24. ESI-HRMS (*m/z*): calcd. for $C_{32}H_{44}NO_5^+$ $[M+H]^+$: 522.3214; found: 522.3206. Purity: 100% by HPLC (A: H_2O; B: acetonitrile, graded: 50–100%), t_R 12.947 min, λ: 400 nm.

3-Hydroxy-9β,13α-dimethyl-2-oxo-24,25,26-trinoroleana-1(10),3,5,7-tetraen-29-oicamide,N-(R)-ethyl 2-propanoate (2)

Red powder; yield, 55%; m.p. 102–104 °C; ^{1}H NMR (300 MHz, $CDCl_3$), δ: 7.04–6.96 (m, 1 H), 6.54 (s, 1 H), 6.41 (d, J = 6.5 Hz, 1 H), 6.36 (s, 1 H), 4.48–4.38 (m, 1 H), 4.08–4.29 (m, 2 H), 2.46 (d, J = 15.3 Hz, 1 H), 2.22 (s, 3 H), 1.60–2.06 (m, 14 H), 1.45 (s, 3 H), 1.35 (d, J = 6.8 Hz, 3 H), 1.26 (d, J = 7.7 Hz, 6 H), 1.17 (d, J = 13.5 Hz, 6 H), 0.88 (m, 1 H), 0.61 (s, 3 H). ^{13}C NMR (75 MHz, $CDCl_3$), δ: 178.35, 177.26, 173.51, 170.24, 164.74, 146.01, 134.03, 127.37, 119.53, 118.03, 117.02, 61.55, 50.88, 47.91, 45.05, 44.27, 39.34, 38.14, 36.30, 34.75, 33.66, 33.45, 31.60, 30.93, 30.80, 29.96, 29.70, 29.44, 28.69, 21.78, 18.55, 18.22, 14.04, 10.25. ESI-HRMS (*m/z*): calcd for $C_{34}H_{48}NO_5^+$ $[M+H]^+$: 550.3527; found: 550.3511. Purity: 99.427% by HPLC (A: H_2O; B: acetonitrile, graded: 50–100%), t_R 15.047 min, λ: 400 nm.

3-Hydroxy-9β,13α-dimethyl-2-oxo-24,25,26-trinoroleana-1(10),3,5,7-tetraen-29-oicamide,N-methyl 3-methyl butyrate (3)

Red powder; yield, 26%; m.p. 96–98 °C; ^{1}H NMR (300 MHz, $CDCl_3$), δ: 7.00 (d, J = 7.0 Hz, 1 H), 6.52 (s, 1 H), 6.32 (t, J = 7.0 Hz, 2 H), 4.42 (dd, J = 8.3, 4.6 Hz, 1 H), 3.67 (s, 3 H), 2.51 (d, J = 12.9 Hz, 1 H), 2.20 (s, 3 H), 2.10 (m, 1 H), 1.64–1.91 (m, 14 H), 1.42 (s, 3 H), 1.25–1.13 (m, 9 H), 0.97 (d, J = 6.1 Hz, 1 H), 0.87 (dd, J = 6.7, 3.5 Hz, 6 H), 0.53 (s, 3 H). ^{13}C NMR (75 MHz, $CDCl_3$), δ: 178.36, 177.76, 172.90, 170.20, 164.77, 146.01, 134.01, 127.38, 119.49, 118.01, 116.99, 56.69, 52.16, 45.07, 44.25, 43.02, 40.66, 39.28, 38.09, 36.27, 34.77, 33.98, 33.35, 31.58, 30.82, 30.65, 30.11, 29.34, 28.66, 21.83, 18.85,18.05, 17.82, 10.24. ESI-HRMS (*m/z*): calcd. for $C_{35}H_{40}NO_5^+$ $[M+H]^+$: 564.3684; found: 564.3680. Purity: 98.056% by HPLC (A: H_2O; B: acetonitrile, graded: 50–100%), t_R 16.247 min, λ: 423 nm.

3-Hydroxy-9β,13α-dimethyl-2-oxo-24,25,26-trinoroleana-1(10),3,5,7-tetraen-29-oic amide, N-methyl4-methylpentanoate (4)

Red powder; yield, 29%; m.p. 102–104 °C; ^{1}H NMR (300 MHz, $CDCl_3$), δ: 7.02 (d, J = 7.1 Hz, 1 H), 6.53 (s, 1 H), 6.35 (d, J = 7.2 Hz, 1 H), 6.19 (d, J = 8.1 Hz, 1 H), 4.55 (s, 1 H), 3.74 (s, 1 H) 3.68 (s, 3 H), 2.50 (d, J = 13.9 Hz, 1 H), 2.23 (s, 3 H), 1.51–1.85 (m, 16 H), 1.45 (s, 3 H), 1.27 (s, 3 H), 1.19 (s, 3 H), 1.14 (s, 3 H), 0.96 (d, J = 5.1 Hz, 1 H), 0.92 (d, J = 6.0 Hz, 6 H), 0.58 (s, 3 H). ^{13}C NMR (75 MHz, $CDCl_3$), δ: 178.34, 177.57, 173.92, 170.15, 164.78, 145.99, 133.98, 127.38, 119.44, 118.03, 117.00, 52.27, 50.41, 45.05, 44.29, 43.00, 42.00, 40.50, 39.27, 38.13, 36.29, 34.79, 33.79, 33.32, 31.63, 30.79, 30.75, 30.08, 29.41, 28.65, 24.87, 22.91, 22.12, 21.85, 18.14, 10.26. ESI-HRMS (*m/z*): calcd. for $C_{36}H_{52}NO_5^+$ $[M+H]^+$: 578.3840; found: 578.3846. Purity: 100% by HPLC (A: H_2O; B: acetonitrile, graded: 50–100%), t_R 19.153 min, λ: 423 nm.

3-Hydroxy-9β,13α-dimethyl-2-oxo-24,25,26-trinoroleana-1(10),3,5,7-tetraen-29-oic amide, N-methyl 4-(methylthio)butanoate (5)

Red powder; yield, 38%; m.p. 116–118 °C; ^{1}H NMR (300 MHz, $CDCl_3$), δ: 7.02 (d, J = 7.1 Hz, 1 H), 6.76 (s, 1 H), 6.66 (d, J = 6.5 Hz, 1 H), 6.54 (s, 1 H), 6.35 (d, J = 7.5 Hz, 1 H), 4.55 (m, 1 H), 3.76 (s, 2 H), 3.73 (d, J = 4.6 Hz, 3 H), 2.66 (d, J = 7.8 Hz, 1 H), 2.47 (m, 3 H), 2.22 (s, 3 H), 2.17 (s, 2 H), 2.09 (s, 3 H), 1.96–1.61 (m, 12 H), 1.45 (s, 3 H), 1.27 (s, 3 H), 1.21–1.14 (m, 6 H), 0.88 (d, J = 6.4 Hz, 1 H), 0.57 (s, 3 H).^{13}C NMR (75 MHz, $CDCl_3$), δ: 178.32, 177.82, 172.78, 170.19, 164.73, 146.01, 134.02, 127.39, 119.53, 118.05, 117.03, 52.56, 51.47, 45.06, 44.26, 43.01, 40.51, 39.31, 38.15, 36.58, 36.28, 34.74, 33.80, 33.39, 31.61, 31.33, 30.81, 30.72, 29.94, 29.41, 28.65, 21.80, 18.15, 15.56, 10.26. ESI-HRMS (*m/z*): calcd for $C_{35}H_{50}NO_5S^+$ $[M+H]^+$: 596.3404; found: 596.3412. Purity: 100% by HPLC (A: H_2O; B: acetonitrile, graded: 50–100%), t_R 15.407 min, λ: 400 nm.

3-Hydroxy-9β,13α-dimethyl-2-oxo-24,25,26-trinoroleana-1(10),3,5,7-tetraen-29-oic amide, N-(R)-methyl -2-phenylacetate (6)

Red powder; yield, 57%; m.p. 144–146 °C; ^{1}H NMR (300 MHz, $CDCl_3$), δ: 7.27 (d, J = 2.2 Hz, 4 H), 6.99 (d, J = 15.7 Hz, 2 H), 6.69 (s, 1 H), 6.47 (s, 1 H), 6.30 (s, 1 H), 5.48 (d, J = 7.1 Hz, 1 H), 3.67 (s, 3 H), 2.32 (s, 1 H), 2.24 (d, J = 15.8 Hz, 3 H), 1.90–1.52 (m, 10 H), 1.39 (s, 3 H), 1.21 (s, 3 H), 1.16 (s, 3 H), 1.10 (s, 3 H), 0.86 (m, 4 H), 0.79 (s, 1 H), 0.41 (s, 3 H). ^{13}C NMR (75 MHz, $CDCl_3$), δ: 178.29, 177.04, 171.90, 170.23, 164.69, 145.98, 136.65, 134.01, 129.07, 128.60, 127.34, 127.25, 119.60, 117.99, 117.09, 55.87, 52.81, 44.99, 44.35, 42.87, 40.13, 39.24, 38.18, 36.29, 34.70, 33.57, 33.11, 31.55, 31.32, 30.75, 29.98, 29.37, 28.61, 21.69, 18.11, 10.27. ESI-HRMS (*m/z*): calcd for $C_{38}H_{48}NO_5^+$ $[M+H]^+$: 598.3527; found: 598.3513. Purity: 100% by HPLC (A: H_2O; B: acetonitrile, graded: 50–100%), t_R 16.447 min, λ: 400 nm.

3-Hydroxy-9β,13α-dimethyl-2-oxo-24,25,26-trinoroleana-1(10),3,5,7-tetraen-29-oic amide, N-(R)-methyl 3-phenylpropanoate (7)

Red powder; yield, 61%; m.p. 128–130 °C; ^{1}H NMR (300 MHz, $CDCl_3$), δ: 7.11 (m, 5 H), 6.99 (s, 1 H), 6.53 (s, 1 H), 6.34 (d, J = 7.1 Hz, 1 H), 6.07 (s, 1 H), 4.63 (d, J = 6.2 Hz, 1 H), 3.71 (s, 3 H), 3.03 (dd, J = 14.3, 5.8 Hz, 2 H), 2.34 (s, 1 H), 2.24 (s, 3 H), 2.06 (d, J = 20.3 Hz, 2 H), 1.66 (dd, J = 53.8, 19.6 Hz, 10 H), 1.43 (s, 3 H), 1.25 (d, J = 12.2 Hz, 6 H), 1.11 (d, J = 11.3 Hz, 6 H), 0.90 (s, 1 H), 0.35 (s, 3 H). ^{13}C NMR (75 MHz, $CDCl_3$), δ: 178.33, 177.21, 172.36, 170.23, 164.73, 146.01, 135.93, 133.95, 129.29, 128.49, 127.37, 127.10, 119.57, 118.00, 116.97, 52.78, 52.33, 45.03, 44.21, 43.01, 40.44, 39.26, 38.14, 37.78, 36.26, 34.72, 33.53, 33.45, 31.59, 30.79, 30.68, 29.97, 29.34, 28.64, 21.81, 18.08, 10.25. ESI-HRMS (*m/z*): calcd. for $C_{39}H_{50}NO_5^+$ $[M+H]^+$: 612.3684; found: 612.3689. Purity: 100% by HPLC (A: H_2O; B: acetonitrile, graded: 50–100%), t_R 17.247 min, λ: 400 nm.

3-Hydroxy-9β,13α-dimethyl-2-oxo-24,25,26-trinoroleana-1(10),3,5,7-tetraen-29-oic amide, N-(S)-methyl 3-phenylpropanoate (8)

Red powder; yield, 72%; m.p. 132–134 °C; ^{1}H NMR (300 MHz, $CDCl_3$), δ: 7.25 (m, 2 H), 7.05(m, 4 H), 6.53 (s, 1 H), 6.34 (d, $J = 6.9$ Hz, 1 H), 6.06 (d, $J = 6.3$ Hz, 1 H), 4.64 (d, $J = 6.4$ Hz, 1 H), 3.71 (s, 3 H), 3.04 (dd, $J = 14.3$, 5.8 Hz, 2 H), 2.34 (s, 1 H), 2.24 (s, 3 H), 1.80 (m, 2 H), 1.61 (m, 12 H), 1.43 (s, 3 H), 1.27 (s, 3 H), 1.11 (d, $J = 11.3$ Hz, 6 H), 0.95 (s, 1 H), 0.35 (s, 3 H). ^{13}C NMR (75 MHz, $CDCl_3$), δ: 178.29, 176.04, 174.18, 170.23, 164.69, 146.01, 134.01, 130.15, 129.24, 128.55, 127.34, 127.18, 119.57, 118.06, 116.97, 53.78, 52.33, 45.03, 44.40, 42.98, 40.15, 39.30, 38.20, 37.89, 36.26, 34.72, 33.53, 33.30, 31.47, 30.80, 30.68, 29.98, 29.34, 28.63, 21.77, 18.24, 10.27. ESI-HRMS (*m/z*): calcd for $C_{39}H_{50}NO_5^+$ $[M + H]^+$: 612.3684; found: 612.3686. Purity: 100% by HPLC (A: H_2O; B: acetonitrile, graded: 50–100%), t_R 17.140 min, λ: 400 nm.

3-Hydroxy-9β,13α-dimethyl-2-oxo-24,25,26-trinoroleana-1(10),3,5,7-tetraen-29-oic amide, N-(S)-dimethyl pentanedioate (9)

Red powder; yield, 60%; m.p. 124–126 °C; ^{1}H NMR (300 MHz, $CDCl_3$), δ: 7.00 (d, $J = 6.8$ Hz, 1 H), 6.65 (d, $J = 6.9$ Hz, 1 H), 6.52 (s, 1 H), 6.33 (d, $J = 7.3$ Hz, 1 H), 4.42 (d, $J = 5.2$ Hz, 1 H), 3.67 (d, $J = 6.4$ Hz, 6 H), 2.37 (dd, $J = 19.5$, 12.2 Hz, 3 H), 2.20 (s, 3 H), 2.12 (m, 3 H), 2.00 (m, 2 H), 1.83 (m, 3 H), 1.61 (s, 8 H), 1.43 (s, 3 H), 1.28–1.12 (m, 9 H), 0.82 (d, $J = 18.1$ Hz, 1 H), 0.54 (s, 3 H). ^{13}C NMR (75 MHz, $CDCl_3$), δ: 178.35, 178.04, 173.57, 172.63, 170.07, 164.71, 146.02, 133.98, 127.40, 119.51, 118.06, 116.99, 52.51, 51.91, 51.62, 45.05, 44.31, 42.99, 40.43, 39.32, 38.13, 36.30, 34.79, 33.73, 33.39, 31.62, 30.82, 30.76, 30.00, 29.94, 29.42, 28.67, 27.10, 21.82, 18.17, 10.25. ESI-HRMS (*m/z*): calcd. for $C_{36}H_{50}NO_7^+$ $[M + H]^+$: 608.3582; found: 608.3571. Purity: 100% by HPLC (A: H_2O; B: acetonitrile, graded: 50–100%), t_R 14.173 min, λ: 423 nm.

3-Hydroxy-9β,13α-dimethyl-2-oxo-24,25,26-trinoroleana-1(10),3,5,7-tetraen-29-oic amide, N-(R)-methyl 2-amino-3–(1 H-imidazol-4-yl)propanoate (10)

Red powder; yield, 31%; m.p. 141–143 °C; ^{1}H NMR (300 MHz, $CDCl_3$), δ: 7.73 (d, $J = 5.6$ Hz, 1 H), 7.49 (s, 1 H), 7.07 (d, $J = 7.1$ Hz, 1 H), 6.85 (d, $J = 20.6$ Hz, 2 H), 6.49 (s, 1 H), 6.35 (m, 1 H), 5.02–4.87 (m, 1 H), 4.48–4.17 (m, 2 H), 3.84 (s, 2 H), 3.68 (s, 3 H), 2.67 (d, $J = 9.3$ Hz, 1 H), 2.23 (s, 3 H), 1.42(m, 3 H), 1.27 (m, 12 H), 1.24 (s, 3 H), 1.12 (d, $J = 11.3$ Hz, 6 H), 0.90 (s, 1 H), 0.50 (s, 3 H). ESI-HRMS (*m/z*): calcd for $C_{37}H_{50}N_3O_5^+$ $[M + H]^+$: 616.3745; found: 617.3752. Purity: 100% by HPLC (A: H_2O; B: acetonitrile, graded: 50–100%), t_R 13.113 min, λ: 423 nm.

3-Hydroxy-9β,13α-dimethyl-2-oxo-24,25,26-trinoroleana-1(10),3,5,7-tetraen-29-oic amide, N-(R)-methyl -3-(1 H-indol-2-yl)propanoate (11)

Red powder; yield, 46%; m.p. 136–138 °C; ^{1}H NMR (300 MHz, $CDCl_3$), δ: 8.37 (s, 1 H), 7.54 (d, $J = 6.9$ Hz, 1 H), 7.39 (d, $J = 7.4$ Hz, 1 H), 7.19 (d, $J = 8.0$ Hz, 1 H), 7.13 (d, $J = 7.6$ Hz, 1 H), 6.98 (s, 3 H), 6.53 (s, 1 H), 6.41–6.27 (m, 2 H), 4.64 (s, 1 H), 3.65 (s, 3 H), 3.25 (s, 2 H), 2.30 (d, $J = 14.5$ Hz, 1 H), 2.20 (s, 3 H), 2.00 (s, 2 H), 1.82 (d, $J = 13.1$ Hz, 2 H), 1.63 (s, 10 H), 1.40 (s, 3 H), 1.23 (d, $J = 17.8$ Hz, 9 H), 1.06 (s, 3 H), 0.87 (d, $J = 6.1$ Hz, 1 H), 0.44 (s, 3 H). ^{13}C NMR (75 MHz, $CDCl_3$), δ: 178.36, 177.55, 172.74, 170.64, 164.97, 146.03, 136.10, 134.34, 127.71, 127.29, 122.76, 122.25, 119.69, 119.37, 118.32, 118.02, 117.23, 121.40, 110.26, 53.69, 52.30, 45.01, 44.27, 43.02, 40.25, 39.24, 38.20, 36.27, 34.74, 33.53, 33.35, 31.59, 31.00, 30.68, 29.89, 29.25, 28.59, 27.45, 21.73, 18.04, 10.27. ESI-HRMS (*m/z*): calcd for $C_{41}H_{51}N_2O_5^+$ $[M + H]^+$: 651.3792; found: 651.3779. Purity: 100% by HPLC (A: H_2O; B: acetonitrile, graded: 50–100%), t_R 15.893 min, λ: 400 nm.

General procedure for the synthesis of compound **12–24**

A mixture of celastrol (45 mg, 0.1 mmol), $NaHCO_3$ (25 mg, 0.3 mmol), and halide derivatives (0.12 mmol) in DMF (4.0 ml) was stirred at 20 °C overnight. After confirming the progress of the reaction by thin-layer chromatography, the reaction mixture was transferred to 5 ml of water with 5 ml EA. The EA layer was washed with water (5 ml × 3) and saline (5 ml × 3) and dried using anhydrous $MgSO_4$. The mixture was then purified by normal-phase column chromatography (PE:EA = 10:1) to obtain the target compounds **12**.

3-Hydroxy-9β,13α-dimethyl-2-oxo-24,25,26-trinoroleana-1(10),3,5,7-tetraen-29-oicacid-(N-phenylacetamiden-1-yl)ethanone (12)

Red powder; yield, 38%; m.p. 90–92 °C; ^{1}H NMR (300 MHz, $CDCl_3$), δ: 7.70 (s, 1 H), 7.51 (d, $J = 7.5$ Hz, 2 H), 7.37 (t, $J = 7.7$ Hz, 2 H), 7.17 (s, 1 H), 6.98 (d, $J = 13.8$ Hz, 1 H), 6.44 (s, 1 H), 6.34 (d, $J = 6.9$ Hz, 1 H), 4.66 (d, $J = 15.2$ Hz, 1 H), 4.53 (d, $J = 15.4$ Hz, 1 H), 2.48 (d, $J = 15.5$ Hz, 1 H), 2.22 (s, 3 H), 2.06 (s, 2 H), 1.75 (s, 3 H), 1.53–1.75 (m, 8 H), 1.44 (s, 3 H), 1.35 (s, 3 H), 1.29 (s, 3 H), 1.16 (s, 3 H), 0.88 (d, $J = 6.7$ Hz, 1 H), 0.56 (s, 3 H). ^{13}C NMR (75 MHz, $CDCl_3$), δ: 178.35, 176.91, 169.02, 164.40, 164.01, 146.01, 136.69, 133.70, 129.23, 127.54, 125.02, 119.85, 119.80, 119.67, 118.24, 116.94, 63.26, 44.93, 44.35, 42.25, 42.77, 40.65, 39.42, 38.24, 36.31, 34.74, 33.39, 32.78, 31.58, 31.07, 30.54, 30.00, 29.90, 28.56, 21.62, 18.80, 10.25. ESI-HRMS (*m/z*): calcd for $C_{37}H_{45}NNaO_5^+$ $[M + Na]^+$: 606.3190; found: 606.3180. Purity: 98.047% by HPLC (A: H_2O; B: acetonitrile, graded: 50–100%), t_R 17.993 min, λ: 220 nm.

3-Hydroxy-9β,13α-dimethyl-2-oxo-24,25,26-trinoroleana-1(10),3,5,7-tetraen-29-oic acid-(4-chlorophenylamino)ethanone (13)

Red powder; yield, 42%; m.p. 110–112 °C; ^{1}H NMR (300 MHz, $CDCl_3$), δ: 7.68 (s, 2 H), 7.46 (d, $J = 8.9$ Hz, 2 H), 7.00 (d, $J = 10.2$ Hz, 2 H), 6.47 (s, 1 H), 6.34 (d, $J = 7.7$ Hz, 1 H), 4.66 (d, $J = 15.8$ Hz, 1 H), 4.50 (d, $J = 15.0$ Hz, 1 H), 2.48 (d, $J = 16.7$ Hz, 1 H), 2.22 (s, 3 H), 1.82–1.57 (m, 12 H), 1.46 (s, 3 H), 1.37–1.27 (m, 9 H), 1.16 (s, 3 H), 0.98 (s, 1 H), 0.55 (s, 3 H). ^{13}C NMR (75 MHz, $CDCl_3$), δ: 178.32, 177.13, 169.27, 164.88, 164.52, 146.02, 135.38, 133.92, 129.91, 129.2, 127.49, 121.80, 119.58, 118.26, 117.73, 63.17, 44.95, 44.17, 42.81, 40.64, 39.38, 38.28, 36.26, 34.68, 33.40, 32.81, 31.56, 31.01, 30.54, 29.94, 29.72, 28.54, 21.61, 18.85, 10.30. ESI-HRMS (*m/z*): calcd for $C_{37}H_{44}ClNNaO_4^+$ $[M + Na]^+$: 640.3800; found: 640.3789. Purity: 100% by HPLC (A: H_2O; B: acetonitrile, graded: 50–100%), t_R 13.460 min, λ: 423 nm.

3-Hydroxy-9β,13α-dimethyl-2-oxo-24,25,26-trinoroleana-1(10),3,5,7-tetraen-29-oic acid-(2-fluorophenylamino)ethanone (14)

Red powder; yield, 28%; m.p. 118–122 °C; ^{1}H NMR (300 MHz, $CDCl_3$), δ: 8.38 (s, 1 H), 8.09 (s, 1 H), 7.17–7.11 (m, 2 H), 7.04–6.96 (m, 2 H), 6.45 (s, 1 H), 6.35 (d, $J = 7.6$ Hz, 1 H), 4.74–4.64 (m, 1 H), 4.55 (t, $J = 8.4$ Hz, 1 H), 2.49 (d, $J = 14.9$ Hz, 1 H), 2.22 (s, 3 H), 2.12–1.55 (m, 14 H), 1.45 (s, 3 H), 1.35 (s, 3 H), 1.29 (s, 3 H), 1.16 (s, 3 H), 0.87 (s, 1 H), 0.57 (s, 3 H). ^{13}C NMR (75 MHz, $CDCl_3$), δ: 178.36, 176.74, 169.13, 164.86, 164.44, 147.73, 146.00, 133.74, 127.53, 125.49, 125.36, 124.89, 121.44, 119.66, 118.24, 116.97, 114.91,

114.66, 63.21, 44.93, 44.24, 42.79, 42.79, 40.68, 39.43, 38.26, 36.30, 34.73, 33.40, 32.67, 31.58, 31.12, 30.53, 29.98, 29.84, 28.57, 21.64, 18.79, 10.24. ESI-HRMS (*m/z*): calcd for $C_{37}H_{44}FNNaO_4^+$[M + Na]$^+$: 624.3096; found: 624.3089. Purity: 100% by HPLC (A: H_2O; B: acetonitrile, graded: 50–100%), t_R 18.900 min, λ: 423 nm.

3-Hydroxy-9β,13α-dimethyl-2-oxo-24,25,26-trinoroleana-1(10),3,5,7-tetraen-29-oicacid-N-(2-methoxyphenyl)acetamide (15)

Red powder; yield, 50%; m.p. 114–116 °C; ^{1}H NMR (300 MHz, $CDCl_3$), δ: 8.53 (s, 1 H), 8.40 (d, *J* = 7.8 Hz, 1 H), 7.15–7.08 (m, 1 H), 7.00 (d, *J* = 8.1 Hz, 2 H), 6.92 (d, *J* = 8.0 Hz, 1 H), 6.46 (s, 1 H), 6.35 (s, 1 H), 4.59 (dd, *J* = 36.9, 15.6 Hz, 2 H), 3.91 (s, 3 H), 2.52 (d, *J* = 15.7 Hz, 1 H), 2.22 (s, 3 H), 2.07–1.59 (m, 14 H), 1.45 (s, 3 H), 1.36 (s, 3 H), 1.29 (s, 3 H), 1.17 (s, 3 H), 0.89 (m, 1 H), 0.57 (s, 3 H). ^{13}C NMR (75 MHz, $CDCl_3$), δ: 178.36, 176.67, 169.96, 164.53, 164.41, 147.73, 146.01, 133.70, 126.67, 124.40, 124.31, 121.39, 119.76, 119.69, 118.22, 116.95, 109.91, 63.26, 55.61, 44.95, 44.31, 42.77, 40.63, 39.43, 38.25, 36.41, 34.69, 33.41, 32.68, 31.62, 33.11, 30.55, 29.91, 29.72, 28.56, 21.63, 18.74, 10.25. ESI-HRMS (*m/z*): calcd for $C_{38}H_{47}NNaO_6^+$ [M + Na]$^+$: 636.3296; found: 636.3284. Purity: 100% by HPLC (A: H_2O; B: acetonitrile, graded: 50–100%), t_R 19.320 min, λ: 423 nm.

3-Hydroxy-9β,13α-dimethyl-2-oxo-24,25,26-trinoroleana-1(10),3,5,7-tetraen-29-oic acid-(4-ethylpiperazin-1-yl)ethanone (16)

Red powder; yield, 51%; m.p. 100–102 °C; ^{1}H NMR (300 MHz, $CDCl_3$), δ: 7.03 (s, 1 H), 6.56 (s, 1 H), 6.37 (d, *J* = 7.1 Hz, 1 H), 4.73 (m, H-1′b, 1 H), 4.52 (m, H-1′a, 1 H), 3.69 (s, 2 H), 3.44 (s, 2 H), 2.48 (m, 7 H), 2.23 (s, 3 H), 2.08–2.21 (m,5 H), 1.60 (m, 8 H), 1.47 (s, 3 H), 1.34 (s, 3 H), 1.28 (s, 3 H), 1.11 (m, 6 H), 1.00 (m, 1 H), 0.55 (s, 3 H). ^{13}C NMR (75 MHz, $CDCl_3$), δ: 178.31, 177.78, 170.40, 164.88, 164.74, 146.30, 134.19, 127.39, 119.57, 118.19, 117.27, 62.68, 52.43, 52.17, 51.98, 45.08, 44.24, 42.97, 40.49, 39.41, 38.34, 36.35, 34.68, 33.59, 32.76, 31.58, 30.82, 30.57, 29.81, 29.58, 28.67, 21.61, 18.76, 11.49, 10.26. ESI-HRMS (*m/z*): calcd. for $C_{37}H_{52}N_2N_aO_5^+$ [M + Na]$^+$: 627.3768; found: 627.3765. Purity: 100% by HPLC (A: H_2O; B: acetonitrile, graded: 50–100%), t_R 14.953 min, λ: 423 nm.

3-Hydroxy-9β,13α-dimethyl-2-oxo-24,25,26-trinoroleana-1(10),3,5,7-tetraen-29-oicacid-(4-phenylpiperazin-1-yl)ethanone (17)

Red powder; yield, 52%; m.p. 118–120 °C; ^{1}H NMR (300 MHz, $CDCl_3$), δ: 7.32 (s, 2 H), 7.04 (d, *J* = 7.1 Hz, 1 H), 6.99 (s, 1 H), 6.92 (d, *J* = 8.1 Hz, 2 H), 6.57 (s, 1 H), 6.37 (d, *J* = 7.2 Hz, 1 H), 4.76 (s, 1 H), 4.58 (s, 1 H), 3.65 (d, *J* = 69.0 Hz, 4 H), 3.18 (d, *J* = 5.4 Hz, 4 H), 2.52 (d, *J* = 16.1 Hz, 1 H), 2.23 (s, 3 H), 1.61–2.11 (m, 14 H), 1.48 (s, 3 H), 1.36 (s, 3 H), 1.29 (s, 3 H), 1.13 (s, 3 H), 1.03–0.98 (m, 1 H), 0.57 (s, 3 H). ^{13}C NMR (75 MHz, $CDCl_3$), δ: 178.31, 177.77, 170.35, 164.86, 150.78, 146.02, 134.17, 129.27, 127.40, 120.76, 119.57, 118.19, 117.24, 116.78, 60.72, 50.88, 49.37, 45.08, 44.49, 44.25, 42.96, 40.50, 39.40, 38.35, 36.35, 34.67, 33.59, 32.76, 31.58, 30.83, 30.58, 29.84, 29.59, 28.67, 21.62, 18.77, 10.27. ESI-HRMS (*m/z*): calcd for $C_{41}H_{52}N_2NaO_5^+$ [M + Na]$^+$: 675.3768; found: 675.3758. Purity: 100% by HPLC (A: H_2O; B: acetonitrile, graded: 50–100%), t_R 19.007 min, λ: 423 nm.

3-Hydroxy-9β,13α-dimethyl-2-oxo-24,25,26-trinoroleana-1(10),3,5,7-tetraen-29-oic acid-(4-benzylpiperazin-1-yl)ethanone (18)

Red powder; yield, 45%; m.p. 110–112 °C; ^{1}H NMR (300 MHz, $CDCl_3$), δ: 7.32 (m, 4 H), 7.04 (d, *J* = 6.8 Hz, 1 H), 6.97 (s, 1 H), 6.55 (s, 1 H), 6.36 (d, *J* = 6.9 Hz, 1 H), 4.73 (d, *J* = 14.3 Hz, 1 H), 4.48 (d, *J* = 14.4 Hz, 1 H), 3.57 (m, *J* = 33.6 Hz, 4 H), 3.36 (s, 2 H), 2.44 (s, 7 H), 2.23 (s, 3 H), 1.60–1.86 (m, 14 H), 1.47 (s, 3 H), 1.34 (s, 3 H), 1.28 (s, 3 H), 1.12 (s, 3 H), 0.87 (m, 1 H), 0.56 (s, 3 H). ^{13}C NMR (75 MHz, $CDCl_3$), δ: 178.30, 177.75, 170.32, 164.85, 164.70, 146.00, 137.46, 134.13, 129.09, 128.35, 127.39, 127.32, 119.56, 118.16, 117.17, 62.81, 60.76, 52.84, 52.47, 45.07, 44.46, 44.25, 42.96, 41.89, 40.49, 39.40, 38.33, 36.35, 34.69, 33.58, 32.77, 31.58, 30.83, 30.57, 29.81, 29.59, 28.67, 21.63, 18.75, 10.26. ESI-HRMS (*m/z*): calcd for $C_{42}H_{54}N_2N_aO_5^+$ [M + Na]$^+$: 689.3925; found: 689.3920. Purity: 100% by HPLC (A: H_2O; B: acetonitrile, graded: 50–100%), t_R 19.833 min, λ: 423 nm.

3-Hydroxy-9β,13α-dimethyl-2-oxo-24,25,26-trinoroleana-1(10),3,5,7-tetraen-29-oic acid-1-morpholinoethanone (19)

Red powder; yield, 46%; m.p. 112–114 °C;^{1}H NMR (300 MHz, $CDCl_3$), δ: 7.04 (d, *J* = 6.7 Hz, 1 H), 6.55 (s, 1 H), 6.37 (d, *J* = 7.3 Hz, 1 H), 4.74 (d, *J* = 14.2 Hz, 1 H), 4.48 (d, *J* = 14.4 Hz, 1 H), 3.84–3.71 (m, 8 H), 3.38 (s, 2 H), 2.50 (d, *J* = 16.6 Hz, 1 H), 2.23 (s, 3 H), 1.60–1.55 (m, 8 H), 1.47 (s, 3 H), 1.35 (s, 4 H), 1.26 (s, 3 H), 1.24 (s, 3 H), 1.13 (s, 3 H), 0.88 (d, *J* = 7.5 Hz, 1 H), 0.55 (s, 3 H). ^{13}C NMR (75 MHz, $CDCl_3$), δ: 178.30, 177.76, 170.30, 165.04, 164.85, 146.01, 134.15, 127.40, 119.56, 118.19, 117.24, 66.74, 60.61, 58.41, 45.06, 44.23, 42.95, 42.06, 40.49, 39.38, 38.35, 36.34, 34.65, 33.57, 32.75, 30.82, 30.57, 29.81, 29.70, 29.59, 28.66, 21.62, 18.77, 18.45, 10.27. ESI-HRMS (*m/z*): calcd for $C_{35}H_{47}NNaO_6^+$ [M + Na]$^+$: 600.3296; found: 600.3285. Purity: 100% by HPLC (A: H_2O; B: acetonitrile, graded: 50–100%), t_R 15.100 min, λ: 423 nm.

3-Hydroxy-9β,13α-dimethyl-2-oxo-24,25,26-trinoroleana-1(10),3,5,7-tetraen-29-oic acid-(1-piperidin-1-yl)ethanone (20)

Red powder; yield, 56%; m.p. 94–96 °C; ^{1}H NMR (300 MHz, $CDCl_3$), δ: 7.02 (d, *J* = 7.0 Hz, 1 H), 6.96 (s, 1 H), 6.54 (s, 1 H), 6.34 (d, *J* = 7.1 Hz, 1 H), 4.72 (d, *J* = 14.2 Hz, 1 H), 4.46 (d, *J* = 14.3 Hz, 1 H), 3.75–3.69 (m,4 H), 3.26 (m, 2 H), 2.49 (d, *J* = 16.2 Hz, 1 H), 2.21 (s, 3 H), 1.54–1.84 (m, 14 H), 1.45 (s, 3 H), 1.26 (m, 6 H), 1.22 (s, 3 H), 1.10 (s, 3 H), 0.86 (d, *J* = 6.4 Hz, 1 H), 0.54 (s, 3 H). ^{13}C NMR (75 MHz, $CDCl_3$), δ: 178.31, 177.78, 170.42, 164.89, 164.48, 146.01, 134.17, 127.38, 119.55, 118.16, 117.19, 61.60, 58.41, 45.08, 44.26, 42.97, 40.47, 39.40, 38.33, 36.37, 34.70, 33.58, 32.77, 31.58, 30.84, 30.57, 29.83, 29.58, 28.68, 26.27, 25.33, 24.37, 21.63, 18.73, 18.45, 10.26. ESI-HRMS (*m/z*): calcd for $C_{36}H_{50}NNaO_5^+$ [M + Na]$^+$: 598.3503; found: 598.3493. Purity: 100% by HPLC (A: H_2O; B: acetonitrile, graded: 50–100%), t_R 17.973 min, λ: 400 nm.

3-Hydroxy-9β,13α-dimethyl-2-oxo-24,25,26-trinoroleana-1(10),3,5,7-tetraen-29-oic acid-(pyrrolidin-1-yl)ethanone (21)

Red powder; yield, 54%; m.p. 109–111 °C; ^{1}H NMR (300 MHz, $CDCl_3$), δ: 7.04 (d, *J* = 7.1 Hz, 1 H), 6.56 (s, 1 H), 6.37 (d, *J* = 4.4 Hz, 1 H), 4.62 (d, *J* = 14.5 Hz, 1 H), 4.39 (d, *J* = 14.6 Hz, 1 H), 3.35 (m, 4 H), 2.52 (d, *J* = 15.9 Hz, 1 H), 2.23 (d, *J* = 2.8 Hz, 3 H), 1.47–1.96 (m, 18 H), 1.47 (s, 3 H), 1.34 (s, 3 H), 1.28 (s, 3 H), 1.12 (s, 3 H), 0.90 (s, 1 H), 0.56 (s, 3 H). ^{13}C NMR (75 MHz, $CDCl_3$), δ: 178.30, 177.89, 170.55, 167.22, 164.90, 146.01, 134.27, 127.36, 119.54, 118.17, 117.26, 62.90, 61.31, 45.89, 45.10, 44.25, 43.01, 40.48, 39.42, 38.33, 36.37, 34.71, 33.58, 32.79, 31.59, 30.80, 30.57, 29.80, 29.57, 28.68, 26.07, 23.88, 21.62, 18.70, 10.26. ESI-HRMS (*m/z*): calcd for $C_{35}H_{47}NNaO_5^+$[M + Na]$^+$: 584.3346; found: 584.3338. Purity: 100% by HPLC (A: H_2O; B: acetonitrile, graded: 50–100%), t_R 15.853 min, λ: 400 nm.

3-Hydroxy-9β,13α-dimethyl-2-oxo-24,25,26-trinoroleana-1(10),3,5,7-tetraen-29-oic acid-(diethylamino-1-yl))ethanone (22)

Red powder; yield, 33%; m.p. 98–100 °C; ^{1}H NMR (300 MHz, $CDCl_3$), δ: 7.14–6.96 (m, 2 H), 6.56 (s, 1 H), 6.37 (d, J = 7.1 Hz, 1 H), 4.71 (d, J = 14.2 Hz, 1 H), 4.48 (d, J = 14.1 Hz, 1 H), 3.38 (dd, J = 14.3, 7.2 Hz, 2 H), 3.22 (dd, J = 14.4, 7.4 Hz, 2 H), 2.53 (d, J = 15.7 Hz, 1 H), 2.23 (s, 3 H), 1.69–2.16 (m, 8 H), 1.60 (s, 3 H), 1.47 (s, 3 H), 1.36 (s, 3 H), 1.29 (s, 3 H), 1.19 (s, 1 H), 1.15 (m, 7 H), 1.00 (m, 2 H), 0.89 (s, 1 H), 0.57 (s, 3 H). ^{13}C NMR (75 MHz, $CDCl_3$), δ: 178.31, 177.91, 170.54, 165.34, 164.93, 146.00, 134.25, 127.35, 119.54, 118.16, 117.22, 60.68, 45.10, 44.24, 43.00, 40.78, 40.45, 40.27, 39.41, 38.35, 36.37, 34.71, 33.57, 32.80, 31.59, 30.79, 30.57, 29.83, 29.57, 28.67, 21.63, 18.71, 14.18, 12.94, 10.28. ESI-HRMS (*m/z*): calcd for $C_{35}H_{49}NNaO_5^+$ $[M+Na]^+$: 586.3503; found: 586.3507. Purity: 100% by HPLC (A: H_2O; B: acetonitrile, graded: 50–100%), t_R 17.320 min, λ: 423 nm.

3-Hydroxy-9β,13α-dimethyl-2-oxo-24,25,26-trinoroleana-1(10),3,5,7-tetraen-29-oic acid-(3-(4-chlorobenzyl)-3 H-1,2,3-triazol-4-yl) methyl (23)

Red powder; yield, 53%; m.p. 98–100 °C; ^{1}H NMR (300 MHz, $CDCl_3$), δ: 7.48–7.29 (m, 5 H), 7.13 (d, J = 8.1 Hz, 1 H), 7.04 (d, J = 6.9 Hz, 1 H), 6.54 (s, 1 H), 6.35 (d, J = 7.1 Hz, 1 H), 5.46 (d, J = 27.5 Hz, 2 H), 5.08 (d, J = 6.4 Hz, 2 H), 2.40 (s, 1 H), 2.22 (s, 3 H), 1.76 (m, 12 H), 1.45 (s, 3 H), 1.26 (d, J = 4.1 Hz, 3 H), 1.12 (d, J = 15.3 Hz, 6 H), 1.00 (s, 1 H), 0.44 (s, 3 H). ^{13}C NMR (75 MHz, $CDCl_3$), δ: 178.27, 178.11, 170.18, 164.81, 146.03, 143.01, 134.77, 134.14, 132.96, 129.31, 129.25, 127.37, 123.47, 119.53, 118.15, 117.22, 57.22, 53.32, 44.99, 44.13, 42.90, 40.39, 39.34, 38.28, 36.30, 34.60, 33.44, 32.77, 31.51, 30.62, 30.53, 29.71, 29.49, 28.60, 21.59, 18.54, 10.27. ESI-HRMS (*m/z*): calcd for $C_{39}H_{46}ClN_3O_4^+$ $[M+H]^+$: 656.3250; found: 656.3233. Purity: 92.00% by HPLC (A: H_2O; B: acetonitrile, graded: 50–100%), t_R 19.337 min, λ: 423 nm.

3-Hydroxy-9β,13α-dimethyl-2-oxo-24,25,26-trinoroleana-1(10),3,5,7-tetraen-29-oic acid-(3-(4-fluorobenzyl)-3 H-1,2,3-triazol-4-yl) methyl (24)

Red powder; yield, 55%; m.p. 102–104 °C; ^{1}H NMR (300 MHz, $CDCl_3$) δ: 7.41 (s, 1 H), 7.19 (s, 2 H), 7.05 (t, J = 6.6 Hz, 5 H), 6.55 (s, 1 H), 6.35 (d, J = 6.7 Hz, 1 H), 5.42 (s, 1 H), 5.32 (d, J = 2.2 Hz, 1 H), 5.15–5.03 (m, 2 H), 2.43 (d, J = 15.0 Hz, 1 H), 2.23 (s, 3 H), 1.77–1.52 (m, 12 H), 1.45 (s, 3 H), 1.26 (s, 3 H), 1.15 (s, 3 H), 1.10 (s, 3 H), 1.01 (s, 1 H), 0.44 (s, 3 H). ^{13}C NMR (75 MHz, $CDCl_3$), δ: 178.28, 178.14, 170.14, 164.81, 146.02, 142.97, 134.09, 129.90, 129.78, 127.39, 123.39, 119.54, 118.13, 117.13, 116.27, 115.98, 57.24, 53.34, 45.00, 44.14, 42.91, 40.40, 39.34, 38.29, 36.30, 34.62, 33.45, 32.77, 31.53, 30.53, 29.71, 29.50, 28.60, 21.60, 18.54, 13.75, 10.27. ESI-HRMS (*m/z*): calcd for $C_{39}H_{47}FN_3O_4^+$ $[M+H]^+$: 640.3545; found: 640.3543. Purity: 100% by HPLC (A: H_2O; B: acetonitrile, graded: 50–100%), t_R 18.140 min, λ: 400 nm.

Anticancer assay

The anti-proliferative activity of the title compounds against the a panel of eight different human cancer cell lines viz. gastric (AGS), differentiation of advanced gastric (MGC-803), colorectal (HCT-116), differentiation of Early gastric (SGC-7901), liver (BEL-7402), Lung (A549), liver (HepG2) and cervix (HeLa) cell lines were evaluated using a standard MTT-based colorimetric assay.

All cell lines were obtained from the Key Laboratory of Natural Resources and Functional Molecules of the Changbai Mountain (Yanbian University) and maintained in Dulbecco's modified Eagle's medium (DMEM) and RPMI Media 1640 (RPMI1640), supplemented with 10% foetal bovine serum (FBS) at 37 °C in a humidified atmosphere containing 5% CO_2.

MTT assay

Cells were plated in 96-well plates at appropriate densities to ensure exponential growth throughout the experimental period (9×10^3 cells per well), and then allowed to adhere for 24 h. Cells were then treated for 48 h with four serial concentrations (1, 10, 50, and 100 μM) of each compound. Taxol was used as a positive control. After 48 h of incubation, 10 μL of MTT solution were added to each well to a final concentration of 2 mg mL^{-1}. Plates were then incubated for a further 4 h. After incubation, the MTT solution was removed and 150 μL of DMSO were added to each well for coloration. The plates were shaken vigorously for 10 min at room temperature to ensure complete solubilisation. The optometric density (OD) was read on a microplate reader (ELx800, BioTek, Highland Park, Winooski, VT, USA) at 492 nm, and the data were subsequently analysed. The percentage of cell growth inhibition was calculated from the following equation:

$$\text{Inhibitory rate}(\%) = [1-(OD_{treated}-OD_{blank})/(OD_{control}-OD_{blank})] \times 100.$$

Analysis for cell cycle by flow cytometry

AGS cells were plated in 96-well plates (5.0×10^5 cells per well) and incubated at 37 °C for 12 h. Exponentially growing cells were then incubated with compound **11** at different concentrations (0.5, 1.0, and 5.0 μM). After 48 h, untreated cells (control) or cells treated with compound **11** were centrifuged at 1000 rpm for 10 min, and then fixed in 70% ethanol at −20 °C for at least 24 h. The cells were subsequently resuspended in phosphate-buffered saline (PBS) containing 0.1 mg mL^{-1} RNase A and 5 μg mL^{-1} propidium iodide (PI). The cellular DNA content for the cell cycle distribution analysis was measured by flow cytometry using a FACS Calibur flow cytometer with Cell Quest software (Becton-Dickinson, Franklin Lakes, NJ), plotting at least 30 000 events per sample. The percentage of cells in the G1, S and G2 phases of the cell cycle were determined using the ModFit LT V4.0 software package (Verity Software, Topsham, ME).

Analysis for apoptosis by flow cytometry

Apoptosis was detected using an Apoptosis Detection Kit (Invitrogen, Eugene, OR). In brief, cells were cultured in 96-well plates (5.0×10^5 cells per well) and incubated at 37 °C for 12 h. Cells with exponential growth were then incubated with compound **11** at different concentrations (0.1, 1.0, and 5.0 μM). Following 48 h of incubation, the cells were collected, washed twice with PBS and once with 1 × binding buffer, and then stained with 5 μM of annexin V-FITC and 2.5 μM of PI (5 mg mL^{-1}) in 1 × binding buffer for 30 min at 20 °C in the dark. Apoptotic cells were enumerated using a FACSCalibur flow cytometer with Cell Quest software (Becton–Dickinson)

Docking study

The molecular docking study was performed using Discovery Studio (DS) 2017. The ligand and protein were prepared, hydrogen was added and water molecules were deleted by DS Server. The result of docking was treated with DS Client. In this study, the

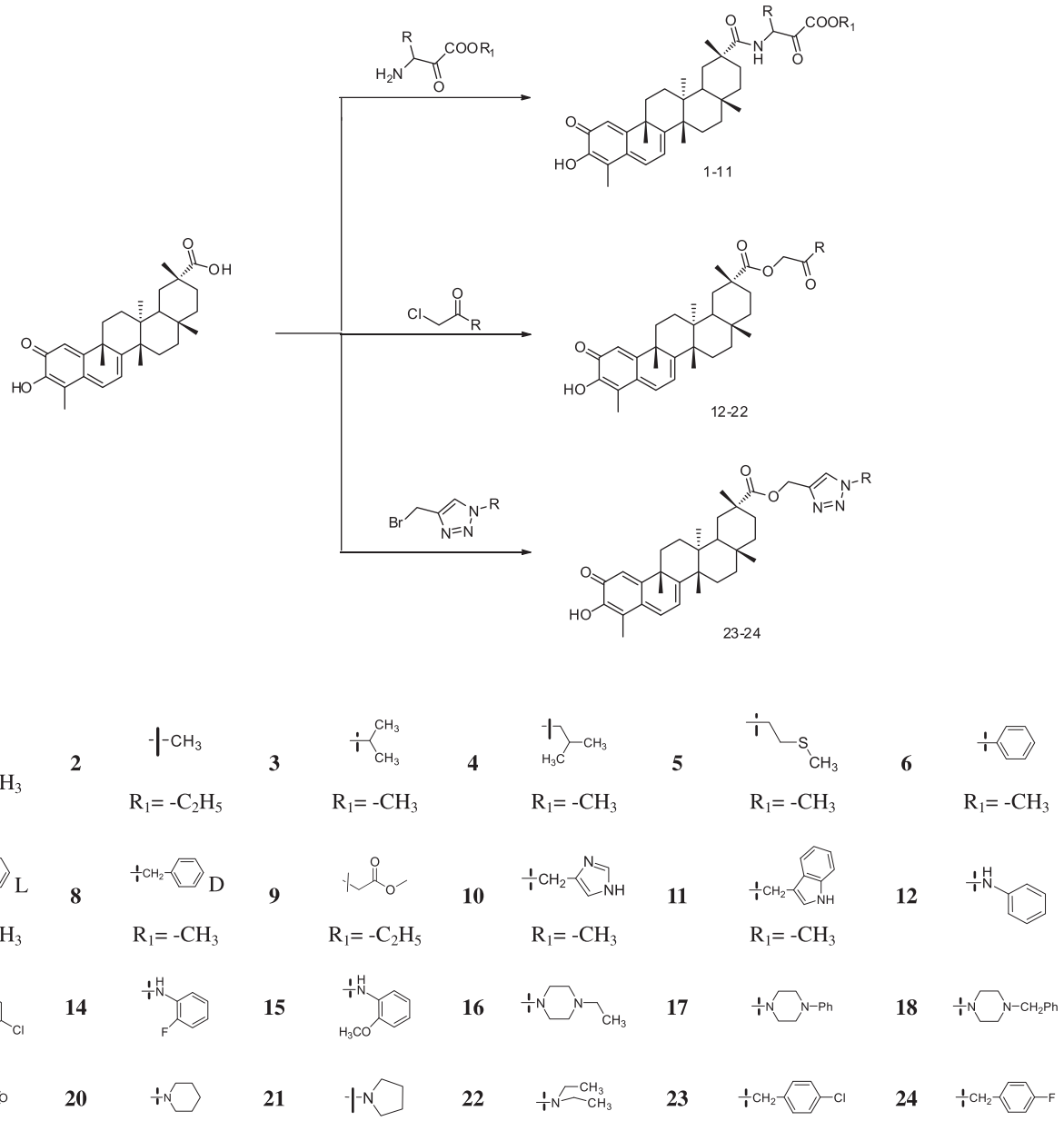

Scheme 1. Synthesis of celastrol derivatives (1–24).

crystal structure of Casepase-3 complex (1GFW) was chosen for docking. The xyz coordinates (37.6468, 33.5653, 27.9733, radius 8.12325 Å) of protein residues were defined as the binding site sphere. The protocol, Dock Ligant (LibDock) was used to perform the docking. The output poses of the ligands generated were analysed based on the LibDockScore function.

Results and discussion

Chemistry

The reaction occurred mainly at the 20th position of celastrol (Scheme 1). Compounds **1**–**11** were obtained by treating celastrol with different amino acids under the catalysis of $NaHCO_3$ in anhydrous DMF, with 26–61% yield. Compounds **12**–**22** were obtained by an amide condensation reaction catalysed by EDC·HCl, HOBt, and TEA in anhydrous CH_2Cl_2, with 33–56% yield. Compounds **23** and **24** were prepared by treating celastrol with phenylbromostannyl. The intermediate 4-(bromomethyl)-1-(4-substituted-benzyl)-1 *H*-1,2,3-triazole was formed by the interactions between 1-(azidomethyl)-4-substituted-benzene and propargyl bromide and $CuSO_4{\cdot}5H_2O$ and VC-Na, respectively.

In vitro *anticancer activity*

All synthesised compounds were evaluated for their anticancer activities *in vitro* against AGS, MGC-803, SGC-7901, HCT-116, A549, HeLa, BEL-7402, and HepG-2 cell lines. The activity of celastrol was used as reference. Cells were allowed to proliferate in presence of the test compounds for 48 h, and the results are presented as IC_{50} values (Table 1). Most of the synthesised compounds showed highly significant antiproliferative effects. Among them, compounds **1**, **2**, **3**, **4**, **6**, **8**, **9**, **10**, **11**, **15**, **17**, **19**, **20**, **21**, **22**, and **24** showed potent inhibitory activities ($IC_{50} \leq 1\,\mu M$; for compounds **8**, **9**, **10**, **11**, **17**, **19**, **20**, **21**, **22**, and **24**, $IC_{50} = 0.74$, 0.72, 0.75, 0.44, 0.75, 0.68, 0.85, 0.88, 0.49, and 0.97 μM, respectively, against AGS cells; for compounds **15** and **22**, $IC_{50} = 0.71$, and 0.78 μM, respectively, against MGC-803 cells; for compounds **8**, **11**, **17**, **20**, and **22**,

Table 1. Anticancer effects of compounds **1**–**24** as analysed by the MTT assay.

	(μM) IC_{50}							
Compd.	AGS	MGC-803	HCT-116	SGC-7901	BEL-7402	A549	HELA	HEPG-2
1	1.05	3.13	1.67	1.78	0.89	1.64	1.89	0.85
2	1.02	2.47	1.48	1.63	0.81	1.62	1.65	1.03
3	1.38	33.16	3.31	2.01	1.36	2.00	2.49	0.9
4	1.01	2.4	2.83	1.53	0.6	1.99	0.73	0.66
5	8.06	9.52	9.67	21.25	2.62	10.33	1.02	4.63
6	1.29	2.19	2.23	1.75	0.68	2.39	1.05	0.88
7	28.04	14.92	3.52	25.82	1.82	6.81	21.47	7.37
8	0.74	1.33	0.90	1.47	0.71	0.96	1.27	0.97
9	0.72	2.46	1.30	1.91	1.19	2.02	1.26	1.39
10	0.75	6.28	5.26	5.89	2.44	3.59	3.65	2.47
11	0.44	1.03	0.78	1.66	0.63	1.22	2.63	0.76
12	0.49	0.78	0.85	1.52	0.98	2.06	0.62	1.02
13	1.93	1.30	2.7	1.57	3.5	2.15	2.83	1.82
14	1.42	1.07	0.93	1.95	1.61	3.81	1.67	4.65
15	2.28	1.57	1.68	2.15	1.91	5.23	3.61	5.83
16	1.09	1.70	1.33	4.14	1.98	1.72	1.08	1.19
17	0.75	1.19	0.88	1.81	1.14	0.91	0.815	0.91
18	1.35	1.69	2.00	4.19	2.35	1.77	1.31	1.18
19	0.68	1.81	1.38	2.54	1.18	2.23	2.25	1.00
20	0.85	1.18	0.84	2.14	1.19	1.71	0.75	0.84
21	0.88	2.34	1.76	1.94	2.27	2.26	2.22	1.43
22	1.10	2.16	1.98	5.39	4.16	3.53	1.84	1.56
23	0.97	2.95	5.23	4.81	4.89	3.52	2.66	2.19
24	5.66	5.77	12.25	61.71	–	54.94	23.47	–
Celastrol	1.46	4.55	3.43	5.71	4.05	3.02	1.51	1.31

IC_{50} = 0.90, 0.78, 0.88, 0.84, and 0.85 μM, respectively, against HCT-116 cells; for compounds **1**, **3**, **6**, **8**, **11**, and **22**, IC_{50} = 0.89, 0.81, 0.60, 0.68, 0.71, 0.63, and 0.98 μM, respectively, against BEL-7402 cells; for compounds **8** and **17**, IC_{50} = 0.96 and 0.91 μM, respectively, against A549 cells; for compounds **3**, **17**, **20**, and **22**, IC_{50} = 0.73, 0.82, 0.75, and 0.62 μM, respectively, against HeLa cells; and for compounds **1**, **3**, **4**, **6**, **8**, **17**, **19**, **20**, and **22**, IC_{50} = 0.85, 0.66, 0.90, 0.88, 0.97, 0.76, 1.00, 0.91, and 0.84 μM, respectively, against HepG-2 cells,), which were greater than that of the reference celastrol.

Using structure–activity relationship (SAR) studies, we attempted to demonstrate how the substituent at the 20th carboxylic acid position of celastrol affected its anticancer activity. Celastrol showed good antiproliferative activity. In particular, it showed remarkable antiproliferative effects against AGS, HeLa, and HepG-2 cell lines with IC_{50} values of 1.46, 1.51, and 1.31 μM, respectively. Compounds **1**–**4**, products of reaction with aliphatic amino acid esters, inhibited the proliferation of most of the tumour cell lines to a greater extent than did celastrol. In particular, the inhibitory activity increased significantly in BEL-7402 cell lines. This indicated that the introduction of hydrophobic groups strengthened the antitumor activity, although significant patterns were not established. By introducing a sulphur (S) atom, compound **5** showed lower inhibitory activity than did compound **4** in most of the tumour cell lines. Remarkably, it showed similar antiproliferative activity to that of compound **4** (IC_{50} 0.73 μM) against HeLa cell lines, with an IC_{50} value of 1.02 μM. Thus, we suspected that the S atoms played an important role in antiproliferation in HeLa cells. The screening results of compound **6**–**8** showed that compound **6** had lower antiproliferative activity than did compound **8**; however, compound 6 had better antiproliferative activity against the 8 cell lines tested than did compound **7**. Unexpectedly, the anticancer activity of compound **7** was much lower than that of compound **8**. This raised an uncertainty as to whether space configuration played a more fundamental role in inhibitory potential than did the length of the carbon chain of amino acids during substitution. Compounds **9**–**11** showed considerably higher antiproliferative activity against AGS and BEL-7402 cell lines. Moreover, compound **11** showed the highest anticancer activity against AGS cell lines. It also showed better anticancer activity against HCT-116, BEL-7402, and HepG-2 cell lines than the other compounds. Compound **12**–**15** showed anticancer activities of varying degrees. In general, introduction of aniline groups had a positive influence on the anticancer activity as compared to that of celastrol; however, their inhibitory activities decreased following the introduction of –Cl, –F, $–OCH_3$ groups, respectively. Among compounds **16**–**18**, where the R-position was substituted with different piperazidine derivatives, compound **17**, which had a nitrogen (N) atom linked to the benzene ring directly, showed the highest anticancer activity. Compounds **16** and **18** showed lower activity, as the N atom was linked to the branched alkyl or the benzene ring indirectly. These results indicate that the inhibitory activity considerably improved when the N atom of piperazidine was linked to the benzene ring directly. Compounds **19**–**21**, heterocyclic compounds with an N atom, expressed higher inhibitory activities against AGS, MGC-803, SGC-7901, HCT-116, A549, and BEL-7402 cell lines than did celastrol. In particular, the IC_{50} values of compound **20** and **21** were 3-fold higher than that of celastrol against SGC-7901, HCT-116, and BEL-7402 cell lines. This result indicates that the activity of substituted groups was increasing in the order piperidine > morpholine, pyrrolidine. Compound **22** showed higher inhibitory activity than did celastrol (4.55, 3.43 μM) against MGC-7901 and HCT-116 cell lines with IC_{50} values of 2.16 and 1.98 μM, respectively. These data of compound **23** and **24** suggested that the introduction of 1,2,3-triazole linked to benzyl chloride had a minor influence on the anticancer activity of celastrol.

Compound 11 *induces AGS cell cycle arrest and apoptosis*

In this study, flow cytometry was used to determine whether compound **11**-mediated inhibition of growth and proliferation was associated with apoptosis. AGS cell lines were treated with compound **11** at concentrations of 0.5, 1.0, and 5.0 μM for 48 h, and the results are shown in Figure 1(A). The proportion of cells in the G1 phase increased from 51.66% (control) to 53.77% (0.5 μM), 59.32(1.0 μM) and 60.51% (5.0 μM), and the proportion of cells in the G2 phase decreased from 21.23% (control) to 18.10% (0.5 μM), 17.70% (1.0 μM) and 16.10% (5.0 μM). Although the rate of G1 and G2 phase presented a trend of change with the increase of the concentration of compound **11**, it did not show significant difference. These results indicate that compound **11** may be weaker influence on cell cycle arrest. Next, cell apoptosis analysis was performed to determine whether compound **11** can induce apoptosis of cells. As shown in Figure 1(B), the early stage apoptosis rate of the control group was 5.2%. The early apoptosis rates gradually increased from 8.7%, 14.5% to 19.0% and the late stage apoptosis rates increased from 2.1%, 2.4%, to 18.1% after treatment with 0.1 μM, 1.0 μM, and 5.0 μM of compound **11**, respectively, for 48 h. This suggests that compound **11** induced apoptosis and caused a marked increase in apoptosis in a concentration-dependent manner.

Docking analysis

Apoptosis signalling can be initiated either at the cell surface via a death receptor-induced signalling pathway or within the cell via the release of pro-apoptotic factors[22]. Fan et al. have reported that activation of caspases underlies the apoptotic process induced by celastrol[23]. In all probability, compound **11** as a celastrol derivative

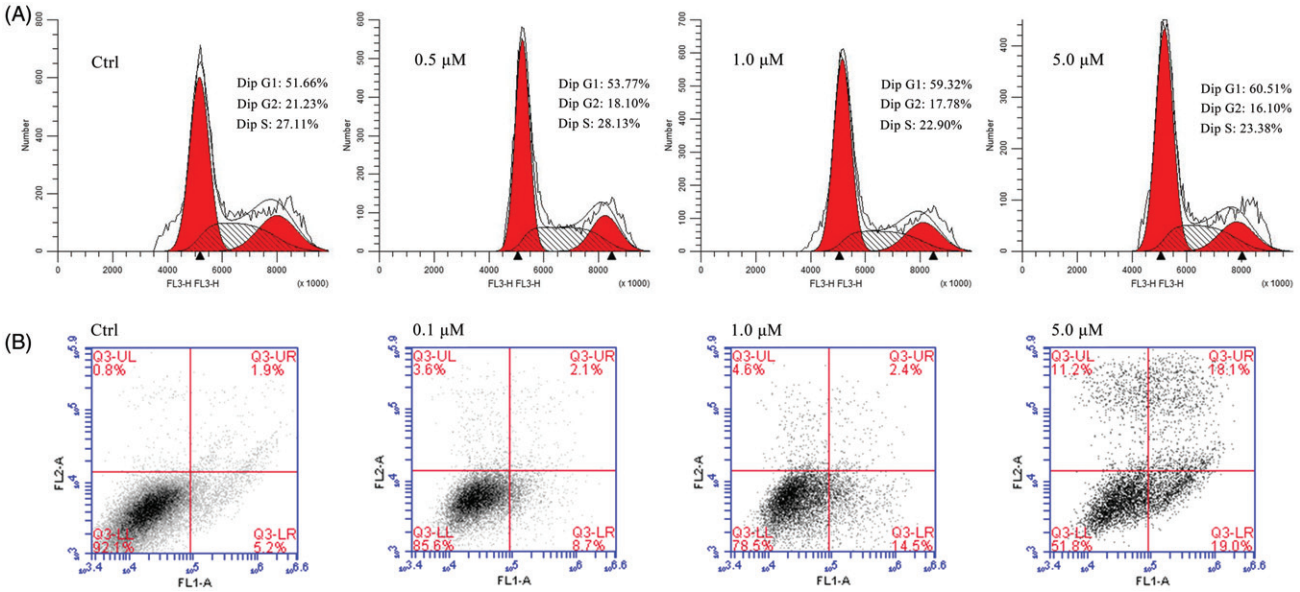

Figure 1. Cell cycle and apoptosis analysis of compound **11** in AGS cells.

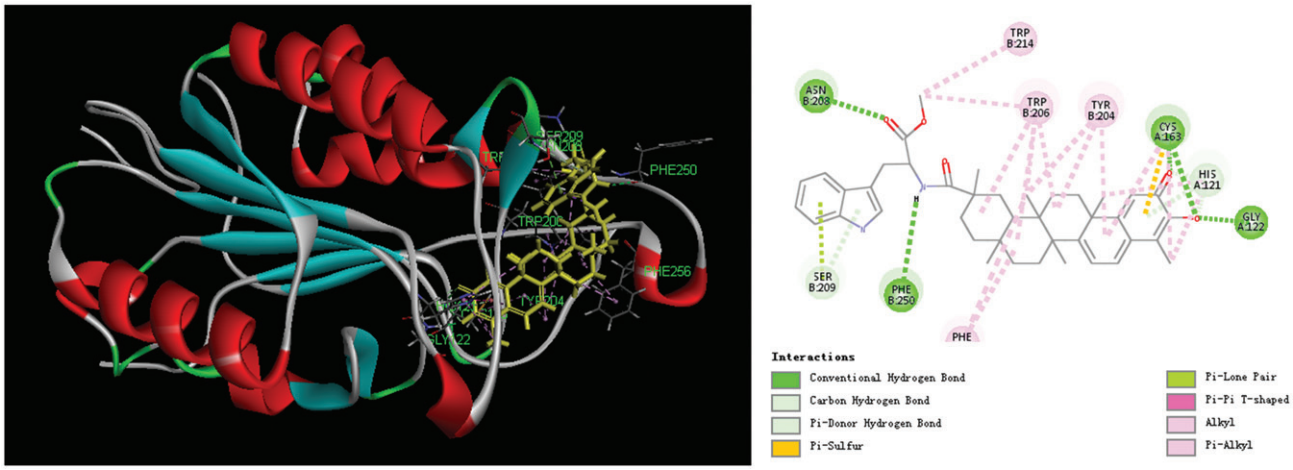

Figure 2. Computer modelling of compound **11** binding to Caspase-3 (1GFW). Compound **11** was colored in yellow.

could induce apoptosis by inducing the activation of caspases. The caspase-3 plays a key role in the apoptotic pathway[24]. To confirm this speculation, in this text, docking simulation was performed to position compound **11** into the caspase-3 (1GFW) active site to determine the probable binding model (Figure 2). The result revealed that five conventional hydrogen bonds and three carbon hydrogen bonds are observed with residue His 121, Gly 122, Cys 163, Asn 208, and Phe 250. Also, the indole ring interacted with the residue Ser 209. This result gives some clue for the mechanism of compound **11** inducing apoptosis by inducing the activation of caspase-3. Therefore, these results indicate that the potent antiproliferative activity of compound **11** possibly involved in inducing apoptosis by inducing the activation of caspase-3.

Conclusions

In summary, we designed and synthesised three series of celastrol derivatives (**1–24**), and evaluated their anticancer effects against eight cancer cell lines (AGS, MGC-803, SGC-7901, HCT-116, A549, HeLa, BEL-7402, and HepG-2). Most of the target compounds exhibited potent inhibitory activity *in vitro*, and the antiproliferative activity of these compounds was screened via the MTT assay. In particular, compound **11** exhibited excellent inhibitory activity against AGS cells, with an IC_{50} value of 0.44 μM. Moreover, it showed higher inhibitory activities against HCT-116, BEL-7402, and HepG-2 cell lines, with IC_{50} values of 0.78, 0.63, and 0.76 μM, respectively. The results of experiments on cell cycle arrest and apoptosis induced by compound **11** suggested that it induced apoptosis in AGS cells. Docking study also revealed the amino acids His-121, Gly122, Asn 208, and Phe 250 were found to be playing crucial role in the binding of compound **11** within the active site of caspase-3. Therefore, the modifications to the 20th position of celastrol in this study were helpful to improve its anticancer activity.

Disclosure statement

We declare that we have no conflict of interest with respect to this study.

Funding

This work was supported by the Natural Science Foundation of Jilin Province [No. 20160101218JC].

References

1. Tozawa K, Sagawa M, Kizaki M. Quinone methide tripterine, celastrol, induces apoptosis in human myeloma cells via NF-κB pathway. Int J Oncol 2011;39:1117–22.
2. Jiang QW, Cheng KJ, Mei XL, et al. Synergistic anticancer effects of triptolide and celastrol, two main compounds from thunder god vine. Oncotarget 2015;6:32790–804.
3. Yu X, Zhou X, Fu C, et al. Celastrol induces apoptosis of human osteosarcoma cells via the mitochondrial apoptotic pathway. Oncol Rep 2015;34:1129–36.
4. Zheng L, Fu Y, Zhuang L, et al. Simultaneous NF-κB inhibition and E-cadherin upregulation mediate mutually synergistic anticancer activity of celastrol and SAHA in vitro and in vivo. Int J Cancer 2014;135:1721–32.
5. Luo DQ, Wang H, Tian X, et al. Antifungal properties of pristimerin and celastrol isolated from *Celastrus hypoleucus*. Pest Manag Sci 2005;61:85–90.
6. Divya T, Dineshbabu V, Soumyakrishnan S, et al. Celastrol enhances Nrf2 mediated antioxidant enzymes and exhibits anti-fibrotic effect through regulation of collagen production against bleomycin-induced pulmonary fibrosis. Chem Biol Interact 2016;246:52–62.
7. Jia Z, Xu C, Shen J, et al. The natural compound celastrol inhibits necroptosis and alleviates ulcerative colitis in mice. Int Immunopharmacol 2015;29:552–9.
8. Yang L, Li Y, Ren J, et al. Celastrol attenuates inflammatory and neuropathic pain mediated by cannabinoid receptor type 2. Int J Mol Sci 2014;15:13637–48.
9. Wang C, Shi C, Yang X, et al. Celastrol suppresses obesity process via increasing antioxidant capacity and improving lipid metabolism. Eur J Pharmacol 2014;744:52–8.
10. Paris D, Ganey NJ, Laporte V, et al. Reduction of beta-amyloid pathology by celastrol in a transgenic mouse model of Alzheimer's disease. J Neuroinflammation 2010;7:17.
11. Tang WJ, Wang J, Tong X, et al. Design and synthesis of celastrol derivatives as anticancer agents. Eur J Med Chem 2015;95:166–73.
12. Jiang F, Wang HJ, Bao QC, et al. Optimization and biological evaluation of celastrol derivatives as Hsp90-Cdc37 interaction disruptors with improved druglike properties. Bioorg Med Chem 2016;24:5431–9.
13. Klaić L, Morimoto RI, Silverman RB. Celastrol analogues as inducers of the heat shock response. Design and synthesis of affinity probes for the identification of protein targets. ACS Chem Biol 2012;7:928–37.
14. Tang K, Huang Q, Zeng J, et al. Design, synthesis and biological evaluation of C6-modified celastrol derivatives as potential antitumor agents. Molecules 2014;19:10177–88.
15. Iwaszkiewicz-Grzes D, Cholewinski G, Kot-Wasik A, et al. Synthesis and biological activity of mycophenolic acid-amino acid derivatives. Eur J Med Chem 2013;69:863–71.
16. Voynikov Y, Valcheva V, Momekov G, et al. Theophylline-7-acetic acid derivatives with amino acids as anti-tuberculosis agents. Bioorg Med Chem Lett 2014;24:3043–5.
17. Moon PD, Kim KY, Rew KH, et al. Anti-fatigue effects of porcine placenta and its amino acids in a behavioral test on mice. Can J Physiol Pharmacol 2014;92:937–44.
18. Hicks RP, Abercrombie JJ, Wong RK, Leung KP. Antimicrobial peptides containing unnatural amino acid exhibit potent bactericidal activity against ESKAPE pathogens. Bioorg Med Chem 2013;21:205–14.
19. Jensen CM, Chow HQ, Chen M, et al. Iminolactones as tools for inversion of the absolute configuration of α-amino acids and as inhibitors of cancer cell proliferation. Eur J Med Chem 2016;114:118–33.
20. Staykova STs, Wesselinova DW, Vezenkov LT, Naydenova ED. Synthesis and in vitro antitumor activity of new octapeptide analogs of somatostatin containing unnatural amino acids. Amino Acids 2015;47:1007–13.
21. Csuk R, Niesen-Barthel A, Schafer R, et al. Synthesis and antitumor activity of ring A modified 11-keto-β-boswellic acid derivatives. Eur J Med Chem 2015;92:700–11.
22. Lee MS, Chao J, Yen JC, et al. Schizandrin protects primary rat cortical cell cultures from glutamate-induced apoptosis by inhibiting activation of the MAPK family and the mitochondria dependent pathway. Molecules 2012;18:354–72.
23. Fan XX, Li N, Wu JL, et al. Celastrol induces apoptosis in gefitinib-resistant non-small cell lung cancer cells via caspases-dependent pathways and Hsp90 client protein degradation. Molecules 2014;19:3508–22.
24. Ahmad K, Balaramnavar VM, Baig MH, et al. Identification of potent caspase-3 inhibitors for treatment of multi- neurodegenerative diseases using pharmacophore modeling and docking approaches. CNS Neurol Disord Drug Targets 2014;13:1346–53.